remote sensing

Article

Spatiotemporal Evolution and Risk Analysis of Land Use in the Coastal Zone of the Yangtze River Delta Region of China

Lingzhi Yin [1], Yafei Wang [2,3,*], Chenglai Sun [4] and Yuxuan Ye [5]

1 School of Computer Science and Technology (School of Artificial Intelligence), Zhejiang Sci-Tech University, Hangzhou 310018, China
2 Key Laboratory of Ocean Space Resource Management Technology, MNR, Hangzhou 310007, China
3 Key Laboratory of Regional Sustainable Development Modeling, Institute of Geographic Sciences and Natural Resources Research, Chinese Academy of Sciences, Beijing 100101, China
4 School of Marine Technology and Geomatics, Jiangsu Ocean University, Lianyungang 222005, China
5 School of Geography, Nanjing Normal University, Nanjing 210023, China
* Correspondence: wangyafei@igsnrr.ac.cn

Abstract: The extensive accumulation of big data, along with the development of a high-performance platform, bridge the gap between the previous inability to provide long-term time series and broad-scale coastal zone monitoring and risk warnings with remote sensing techniques. Based on 20 years of Landsat images from the Google Earth Engine platform, the time series land cover in the coastal zone of the Yangtze River Delta in China was classified. Then, a spatiotemporal clustering method based on grid segmentation was proposed to analyze the spatiotemporal evolution details of artificial surface expansion and the risks of cropland loss and ecological degradation caused by this. The results showed that significant changes have taken place in the quantitative structure and spatial morphology of coastal land use in the past 20 years. The artificial surface maintained a growth trend, increasing by 229%, while cropland decreased by 19%. Natural land showed a fluctuation pattern of "up→down→up". The spatiotemporal details of land use obtained through 1km grid segmentation and clustering analysis were more significant. The artificial surface mainly underwent a progressive spatial expansion along the central urban area and important transportation axes (types III and IV), with the most dramatic changes occurring from 2010 to 2013. Type III cropland loss was the most significant, falling from 75.02% in 2000 to 38.23% in 2020. At the same time, the change in type III water body corresponds to the newly increased area of reclamation, which has decreased by 17% in the past 20 years, indicating that the degradation of coastal natural wetlands was significant. This paper provided a comprehensive diagnosis of coastal land use change, which could help policy makers and implementers to propose more targeted and differentiated coastal development and protection policies.

Keywords: Yangtze River Delta coastal zone; land use; time series clustering; cropland loss; ecological degradation

Citation: Yin, L.; Wang, Y.; Sun, C.; Ye, Y. Spatiotemporal Evolution and Risk Analysis of Land Use in the Coastal Zone of the Yangtze River Delta Region of China. *Remote Sens.* **2023**, *15*, 2261. https://doi.org/10.3390/rs15092261

Academic Editor: Yongjiu Feng

Received: 27 February 2023
Revised: 3 April 2023
Accepted: 23 April 2023
Published: 25 April 2023

1. Introduction

A coastal zone is a zone of transition where land and ocean interact vehemently. It is a dynamic and complex natural system marked by highly intensive space development and utilization that faces heavy resource and environmental pressure and witnesses a mixture of all kinds of conflicts [1–3]. A background of rapid urbanization, substantial population migration to coastal zones and high-intensity human activities have led to an accompanying escalation in the scale and intensity of land development in and utilization of the coastal zone. This has encroached on large amounts of high-quality cropland and natural land, leading to problems such as difficulty in maintaining food security, decline in ecological service functions and loss of biodiversity [4,5]. Long-term coastal land use monitoring data can help to discover and understand the temporal and spatial details of human expansion, as well as the temporal and spatial changes in food loss and ecological degradation caused by human expansion [6,7]. With the open application of remote sensing platforms, such as Google Earth Engine (GEE) along with multiple sources of big data, more possibilities for long-term time series coastal zone studies are made available using free data and high-performance platforms [8–10].

Due to the limitations of remote sensing data accumulation and platform performance, most previous studies on the evolution of coastal land have found it difficult to discover the temporal details and local characteristics of land use evolution in the coastal zone [11,12]. These studies relied on classification-based change detection techniques, which can be divided into three categories. The first category is the post-classification comparison method, or bi-temporal change detection method, which classifies all land use types based on several specific time images or thematic maps, and then calculates characteristics such as the transfer matrix and spatial pattern changes with different temporal classification results [13–15]. The second category of studies, based on multi-temporal image classification results, used various modeling methods, such as feature line fitting, spatial gradient analysis, landscape index and sequence-based clustering, to calculate changes in gradients, the spatial relationships of different types, and global characteristics [16–19]. These two types of studies can only obtain change information at a fixed time point, which makes it difficult to match the most critical change point. The third category is based on the identification and change detection of long-time series remote sensing indices, which can be achieved by reconstructing the growth and change process of target features, such as seasonality, periodicity, or stability. This includes the normalized difference vegetation index (NDVI), kernel NDVI (kNDVI), normalized difference water index (NDWI), normalized difference built-up index (NDBI), automated water extraction index (AWEI), etc., and is commonly used for detecting a change in characteristic features, such as coastal wetlands [20,21], mangroves [22,23], coastal mudflats [24], etc. These studies have all fully capitalized on the long-term time series characteristics of remote sensing images, which can detect key points and details in the temporal dimension. However, they focus more on changes in certain land types than on full-element classifications, which makes it impossible for them to capture the evolution patterns and transfer relationships among different types. As natural material and physical flows occur in land–sea ecological processes, which are extremely complex, long-term time series data could contribute to an accurate evaluation of the negative impacts of human activities [25,26]. Therefore, how to further mine the spatiotemporal information contained in long-term remote sensing images and to quantitatively depict the detailed characteristics of the spatiotemporal evolution of coastal zones is the key issue that this paper attempts to solve.

Based on the GEE platform and multi-source big data, this paper explores the application potential of long-term time series remote sensing multi-source products in monitoring and identifying the evolution patterns of land use in coastal zones. Using the coastal zone of the Yangtze River Delta as the case study area, this paper proposes a spatiotemporal pattern recognition method for land use in the coastal zone based on GEE, which includes the following main steps: (1) based on the long-term Landsat satellite images from the GEE platform, the random forest method is used to conduct a land cover classification; (2) the grid segmentation method is introduced to analyze the spatiotemporal evolution pattern of land use based on time series clustering, with a focus on the spatiotemporal characteristics of cropland loss and ecological degradation caused by the expansion of coastal construction.

2. Material and Methods

Figure 1 shows the overall research framework of this paper. First, based on Landsat images from the GEE platform, combined with VIIRS and SRTM DEM data and spectral data, a random forest algorithm was used to extract land use in the Yangtze River Delta for 20 years; then, a 1 km grid was used to divide the entire research area, and the proportion of different land types within each grid was calculated; and finally, cluster analysis and change point detection were conducted for 20 years of land use types. Finally, spatiotemporal evolution analysis was performed on the clustering results, including global and local, spatiotemporal, and spatial analysis.

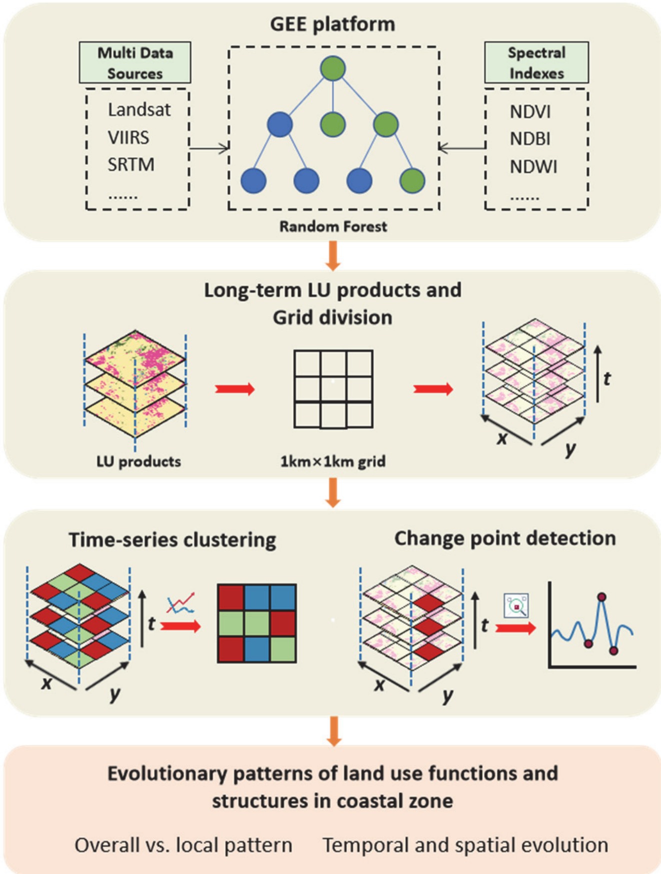

Figure 1. Overall research framework.

2.1. Study Area

The Yangtze River Delta, abbreviated as YRD, is located in the eastern coastal region of China, adjacent to the East China Sea and the Yellow Sea. Its longitude and latitude range from 114°54′ to 123°E and 27°12′ to 35°20′N, respectively. It comprises 41 cities at or above the prefecture level in Jiangsu, Anhui and Zhejiang provinces, and Shanghai city, with a total area of 358,000 km^2 [27]. The topography of the YRD is generally flat and dominated by plains, where the altitude shows a stepwise decreasing trend from south to northeast. The region has a well-developed river network, including important rivers such as the Yangtze River, the Beijing–Hangzhou Grand Canal and the Qiantang River, as well as lakes such as Taihu Lake, Hongze Lake, Chaohu Lake and West Lake [28]. The YRD coastline has a total length of approximately 2409 km, with most of it being silt coast, and featuring extensive and typical tidal flats, with some tidal flats being rich in coastal wetlands. The YRD coastal zone is located in the subtropical monsoon climate zone south of the Qinling Mountains and the Huaihe River, with abundant sunshine throughout the year, hot and rainy summers, cold and dry winters, and distinct four seasons [29].

With the gradual growth in urbanization and development in coastal areas, land use in the Yangtze River Delta coastal zone has changed drastically. This rapid economic development is rooted in the overuse of high-quality cropland, grassland and shoreline resources. This has led to a sharp decrease in the coastal wetland area, the destruction of biological habitats and a severe decline in species resources. The coastal zones have become a hot spot for the contradiction between economic development and ecological protection [30–32]. In the strategic pattern of land development and regional development in China, the Yangtze River Delta coastal zone belongs to the optimized development zone at the national level, the central production zone for agricultural products, and the provincial-level key development zone and key ecological function zone [33]. Meanwhile, in the spatial pattern of the Yangtze River Delta Urban Agglomeration Development Plan (2016–2020), the Yangtze River Delta coastal zone is defined as a coastal development zone, committed to building a marine economic development zone that is in synchronization with ecological construction and environmental protection. With the accelerated promotion of the national marine strategy and the "Belt and Road" initiative, the pressure of coastal land development and resource and environmental protection has multiplied, and the coordination and overall planning of ecological and economic linkages have become the core issue for the sustainable development of coastal land use [34].

The main coastal prefecture-level cities in the Yangtze River Delta were selected as the study area, including Lianyungang city, Yancheng city, Nantong city, Taizhou city, Changzhou city, Wuxi city, Suzhou city, Shanghai city, Jiaxing city, Hangzhou city, Huzhou city, Shaoxing city, Ningbo city, Zhoushan city, Taizhou City, and Wenzhou city. Based on the administrative boundaries, a 10 km buffer zone towards the sea was delineated, as shown in Figure 2.

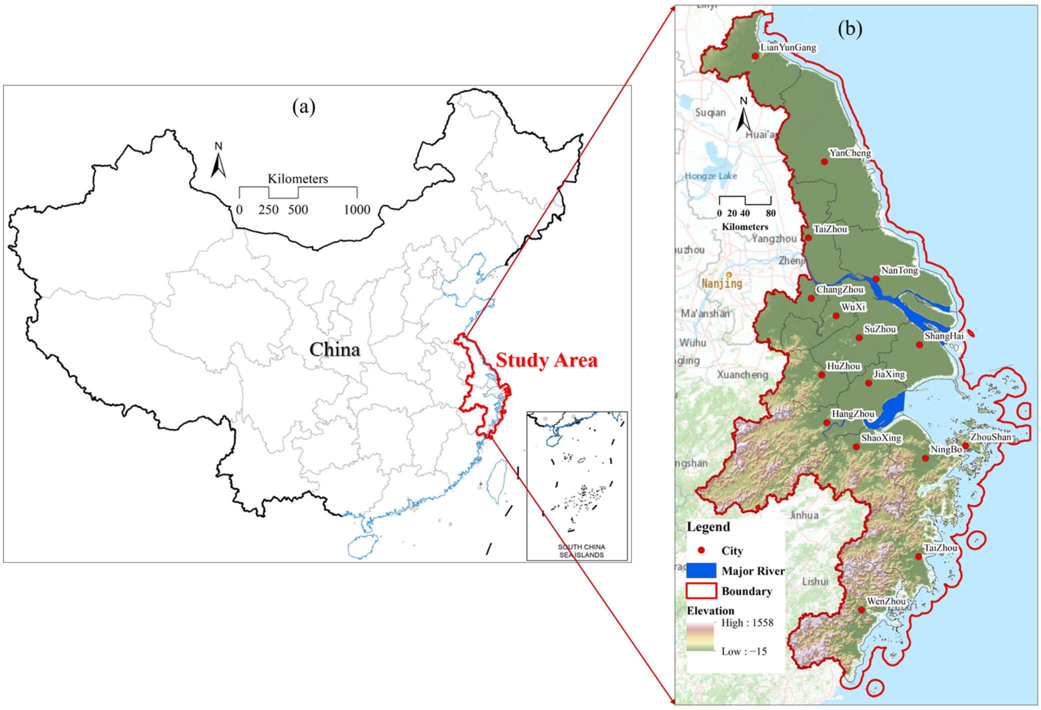

Figure 2. (**a**) The location of the study area; (**b**) the topography and geomorphology of the study area.

2.2. Multi-Source Datasets and Preprocessing

The main data used in this paper are the historical Landsat image data from the GEE platform, including three satellites: Landsat5, Landsat7 and Landsat8. We used the GEE platform to screen the existing Landsat data in the Yangtze River Delta coastal zone between 2000 and 2020 (excluding 2012, due to excessive cloud cover), with the following selection criteria: (1) acquired data for two periods, June to October (vegetation growing season) and November to March of the following year (vegetation senescence season), and (2) cloud cover less than 15%. We obtained 20 years of low-cloud data through screening using pixel-based mosaic image acquisition methods, which contained a total of 3295 images. The source and number of images for each year are shown in Table 1. Using the Landsat series of historical image data, we calculated spectral indices including the NDVI, NDWI, NDBI, enhanced vegetation index (EVI) and radar vegetation index (RVI) after image cropping and stitching, which were used as feature variables for subsequent big data classification using random forest. In addition, the visible infrared imaging radiometer suite (VIIRS), digital elevation from the data shuttle radar topography mission (SRTM), and climate data, including precipitation, temperature, and accumulated temperature, were also included in the feature vector for subsequent classification. Among these, VIIRS nighttime light data (Nighttime Day/Night Band Composites Version 1) was mainly used to distinguish between urban and non-urban areas, and is a monthly average radiation composite image of nighttime data from the day/night band (DNB) of the VIIRS. The SRTM digital elevation data derives from the US Land Processes Distributed Active Archive Center, and the voids have been filled using open-source data (ASTER GDEM2, GMTED2010 and NED). Climate data were obtained from the FLDAS data, an abbreviation for the Famine Early Warning Systems Network (FEWS NET) Land Data Assimilation System. The spatiotemporal resolution of the above data is shown in Table 2.

Table 1. Number and source of images obtained for each year.

Year	Landsat 5	Landsat 7	Landsat 8	Total
2000	72	94	/	166
2001	105	104	/	209
2002	91	115	/	206
2003	87	101	/	188
2004	97	79	/	176
2005	55	99	/	154
2006	82	94	/	176
2007	42	78	/	120
2008	59	75	/	134
2009	63	77	/	140
2010	94	110	/	204
2011	18	61	/	79
2013	/	95	99	194
2014	/	84	89	173
2015	/	80	87	167
2016	/	74	75	149
2017	/	89	94	183
2018	/	75	80	155
2019	/	73	101	174
2020	/	73	75	148
Total	865	1730	700	3295

Table 2. Spatiotemporal resolution of datasets.

Dataset	Spatial Resolution	Temporal Resolution
Landsat 5/7/8	30 m	Per 16 days
VIIRS Nighttime Day/Night Band Composites Version 1	463.83 m	Monthly
FLDAS	11,132 m	Monthly
SRTM DEM	30 m	Not applicable

In terms of sample points selection, with the help of Landsat images in the Google Earth History Archive, sample data of 20 years were obtained through a year-by-year comparison. That is, we obtained training samples in 2020, then switched to historical images in 2019 to check whether the features had changed, and then performed category replacement and adjustment on the samples. This sample selection strategy ensures the continuity and stability of the sample selection process as much as possible. Based on this strategy, 1122 high-quality sample points were obtained per year.

2.3. Research Methods

2.3.1. Time Series Classification of Land Use in the Coastal Zone

A classification and grading index system for the coastal zone was established based on the characteristics of human development and natural ecosystems in coastal zones and by referring to the previous literature [35–37]. The first-level classification included three types of land use: construction land, agricultural land and natural land, with natural land divided into green vegetation (mainly including forests, shrubs and grasslands), water, and unused land, while construction land refers to an artificial surface and agricultural land refers to cropland. First, using historical images in GEE, the sample points of different land use types were selected year by year, with 80% of the sample points being used as a training set and 20% being used as the validation set. Then, according to the characteristics of the study area, the NDVI, NDBI, NDWI and all spectral features that can be calculated on the GEE platform were calculated as feature variables, combined with VIIRS nighttime light data and SRTM DEMs to compare the accuracy of the results of the different combinations of feature variables. After the training was completed, the images were classified year by year. Finally, using the validation sample, the initial accuracy of each year's land use classification results was evaluated in order, and the overall accuracy and kappa coefficient were calculated as the initial accuracy evaluation indicators based on the average of these years.

2.3.2. Land Use Transfer Network and Change Measurement in Coastal Zone

The spatiotemporal evolution process of land use includes not only a change in the amounts and spatial form, but also a change in the transfer direction between land use types. With the different development periods of the study area, there will be differences in amounts, transfer direction and speed, and the spatial form of land use types affected by the natural evolution, social and economic development, and policy planning. In order to comprehensively describe the development and utilization characteristics of different land use types, the transfer characteristics of land use types in the Yangtze River Delta coastal zone from 2000 to 2020 were taken as the analysis object. Different land use types experienced changes in terms of "transfer out", "transfer in", or "maintain unchanged" after the 20 years of development and evolution which had been occurring since 2000, but the total area of land ecosystem stayed balanced. The Sankey diagram, also known as the Sankey energy diversion or balance diagram, was applicable to the visual analysis of a specific flow conversion, which was composed of edges, nodes and energy. Among them, nodes represented different land use types, edges represented flowing data, and flows represented specific values of flowing data. The width of the edges was proportional to the flow, and the sum of the branch widths at the beginning and end followed the principle of energy conservation. The transfer characteristics of a certain land class type could be represented by "the land use type, the amount of transfer, and the land use type transferred to". Therefore, the Sankey diagram was selected to show the characteristics of land use transfer visually, comprehensively and concretely in the study area over the past 20 years. It included the relative proportion of the land use type area at the beginning and end of each period, the direction and amount of land use type transfer, the transfer contribution rate (the percentage of "transfer-out" or "transfer-in" in the net conversion area), and the transfer change rate.

In addition, the annual change rate and dynamic degree index were used in this paper to comprehensively measure the change rate and intensity of land use type A in a certain period [38,39]. The annual change rate had positive and negative values, reflecting the annual expansion rate or annual contraction rate of land use type A in the study area corresponding to the time period. The dynamic degree index reflected the intensity of a specific land use type A change in the study area corresponding to the time period. For a certain land use type A, the annual change rate and dynamic degree index were calculated as follows:

$$K = \frac{U_b - U_a}{U_a} \times \frac{1}{t} \times 100\% = \frac{\Delta U_{in} - \Delta U_{out}}{U_a} \times \frac{1}{t} \times 100\% \tag{1}$$

$$D = \frac{\Delta U_{in} + \Delta U_{out}}{U_a} \times \frac{1}{t} \times 100\% \quad (2)$$

where K and D represent the annual change rate and dynamic degree index of land use type A, respectively. U_a and U_b, respectively, represent the initial area and final area of land use type A in a certain period (km^2). ΔU_{in} is the total area transferred from other land use types to land use type A, namely, the new area (km^2). ΔU_{out} is the total area transferred from land use type A to other land use types, namely, the loss area (km^2). T is the time period.

2.3.3. Spatiotemporal Evolution of Cropland Loss and Ecological Degradation in the Coastal Zone

After obtaining long-term time series land use classification data, to further analyze the evolution patterns and change modes of coastal cropland loss and ecological degradation, a spatial grid of 1 × 1 km was created, and all the grid data for each year were integrated into this grid cell for calculation of the area proportion index. Then, each year's land use type's area proportion was merged in a fully connected manner over time and space, forming a feature vector of land use type area proportion with a time step of 1 year. Finally, due to the large sample size and high feature dimension, the FCM clustering (fuzzy c-means clustering) algorithm was used to perform clustering analysis on the spatiotemporal evolution process of artificial surfaces, cropland and natural land in the long-term time series classification data of the coastal zones in the Yangtze River Delta after a comprehensive consideration of the calculation time and clustering effects.

The FCM algorithm is a fast-clustering algorithm proposed by Dunn and Bezdek, which introduces a fuzzy factor to overcome the binary limitation of the K-means clustering algorithm [40,41]. The FCM algorithm is a clustering algorithm that uses membership degrees to determine the degree to which each data point belongs to a certain cluster. It divides n objects into c groups and then calculates the clustering center of each group. The membership degree $u_{ki} \in [0,1]$ is used to determine the degree to which the sample belongs to each cluster, and it satisfies the following:

$$\sum_{k=1}^{c} u_{ki} = 1(i = 1, 2, ...n) \quad (3)$$

where u_{ki} represents the membership degree of sample i belonging to cluster k. The FCM algorithm finds the membership matrix U and the clustering center c that minimizes the objective function J. The objective function is expressed as follows:

$$J_m(U, c) = \sum_{i=1}^{n} \sum_{k=1}^{c} (u_{ki})^m ||x_i - c_k||_A^2 \quad (4)$$

where m is a weighted index that plays an important role in adjusting the fuzziness of the clustering. Without special requirements, the interval median value m = 2 is a good choice. U is the fuzzy c partition of x_i, u_{ki} is the membership degree of sample x_i belonging to cluster k, and $||x_i - c_k||_A^2$ is the Euclidean distance between sample A and clustering centroid k. The iterative equations of the cluster center v and the dependency degree u are shown as follows:

$$v_i = \frac{\sum_{j=1}^{n} u_{ij}^m x_j}{\sum_{j=1}^{n} u_{ij}^m} (i = 1, 2, 3 \cdots n) \quad (5)$$

$$u_{ij} = \frac{1}{\sum_{k=1}^{c} \left(\frac{d_{ij}}{d_{kj}}\right)^{\frac{2}{m-1}}} (i = 1, 2, 3 \cdots n) \quad (6)$$

where d_{ij} is equal to $||x_i - c_k||_A^2$.

The clusters generated by clustering are a set of data objects that are similar to each other within the same cluster and different from objects in other clusters; that is, the units in the same cluster follow the same land use spatiotemporal evolution pattern. Therefore, the spatiotemporal evolution pattern corresponding to each cluster can be obtained by calculating each cluster's average area proportion value in each year. At the same time, we used a piecewise linear trend function to fit the area proportion value of each cluster in each year, and the change in the slope of different inflection points was used to divide the different land use clustering categories into periods [42]. The computation method is shown below:

$$g(t) = \left(k + \alpha(t)^T\delta\right)t + \left(m + \alpha(t)^T\gamma\right) \tag{7}$$

where k is the growth rate, δ has the rate adjustments, m is the offset parameter and γ is the rate adjustments at the changepoint.

3. Results

3.1. Spatiotemporal Evolution Characteristics of Land Use in the Coastal Zone

An accuracy assessment was conducted and the results showed that the kappa coefficients of the classification result from 2000 to 2020 ranged from 0.9020 to 0.9584, and the overall accuracy was 92.47% to 96.85%. The average kappa coefficient was 0.9247, and the average overall accuracy was 94.33%. The overall classification accuracy was high enough to meet the needs of a subsequent analysis. The overall spatial pattern of land use in the Yangtze River Delta coastal zone showed a north–south division, with agriculture being dominant in the north and forests in the south, as shown in Figure 3. Artificial surface plots were scattered throughout. In 2000, the area of cropland in the Yangtze River Delta coastal zone was 72,210.34 km^2, accounting for a large proportion at 44.97% of the total area, mainly distributed in the coastal plain areas of Jiangsu Province, Shanghai and the northern part of Zhejiang Province. The scale of the artificial surface was relatively small, with a total area of 5774.82 km^2, accounting for only 3.60% of the total area, mainly concentrated in central urban areas such as Shanghai, Suzhou, Hangzhou and Ningbo. The area of natural land is 82,582.5951 km^2, accounting for the largest proportion at 51.43% of the total area. It is mainly located in the southeast and southwest parts of Zhejiang Province. After 20 years of development, the spatial landscape of the Yangtze River Delta coastal region has changed significantly, with the artificial surface increasing to 18,999.23 km^2, accounting for 11.84%, and the proportion of cropland decreasing to 58,224.06 km^2, accounting for 36.27%. Natural land has slightly increased to 83,291.59 km^2, accounting for 51.89%. The overall spatial pattern of land use showed that artificial land patches were scattered and developed throughout. Local explosive expansion occurred, while cropland patches were gradually shrinking. Scattered patches have become increasingly evident, especially since 2010, when new artificial surface patches gradually formed tiny plots scattered throughout the Yangtze River Delta coastal zone, particularly in Shanghai and the Hangzhou Bay coastal zone. In terms of dynamic changes in land use, in these regions the artificial surface changed the most, followed by cropland and natural land.

In Figure 4, a Sankey diagram is used to visualize how different land use types converted, and to what extent, in the study area. Overall, from 2000 to 2020, the main land use change in the study area showed the following trend: artificial surface increased rapidly and unceasingly, cropland was lost continuously, mainly converted to artificial surface, and natural land increased slightly, with fluctuations. The artificial surface area increased by 13,224.40 km^2, resulting in a high growth rate of 229%. There were obvious differences in the expansion rate during different periods. The expansion of artificial surface was most significant from 2010 to 2015, with an increase in the proportion of 4.07%, while from 2000 to 2005, the expansion of artificial surface only increased by 1.71%. The artificial surface was mainly converted from cropland, which ranks first among all other types converted to artificial surface. This was mainly due to the accelerated urbanization and the gradual rise of coastal industries in the study area, which encroached on a large amount of high-quality cropland and caused a serious loss of cropland. Natural land showed an overall fluctuating trend of "increase–decrease–increase". The natural land area increased from 2000 to 2005, 2010 to 2015, and 2015 to 2020. In comparison, from 2005 to 2010, the amount of natural land converted into cropland was more than that in the opposite direction, which may be related to China's frequent protection policies for coastal zones.

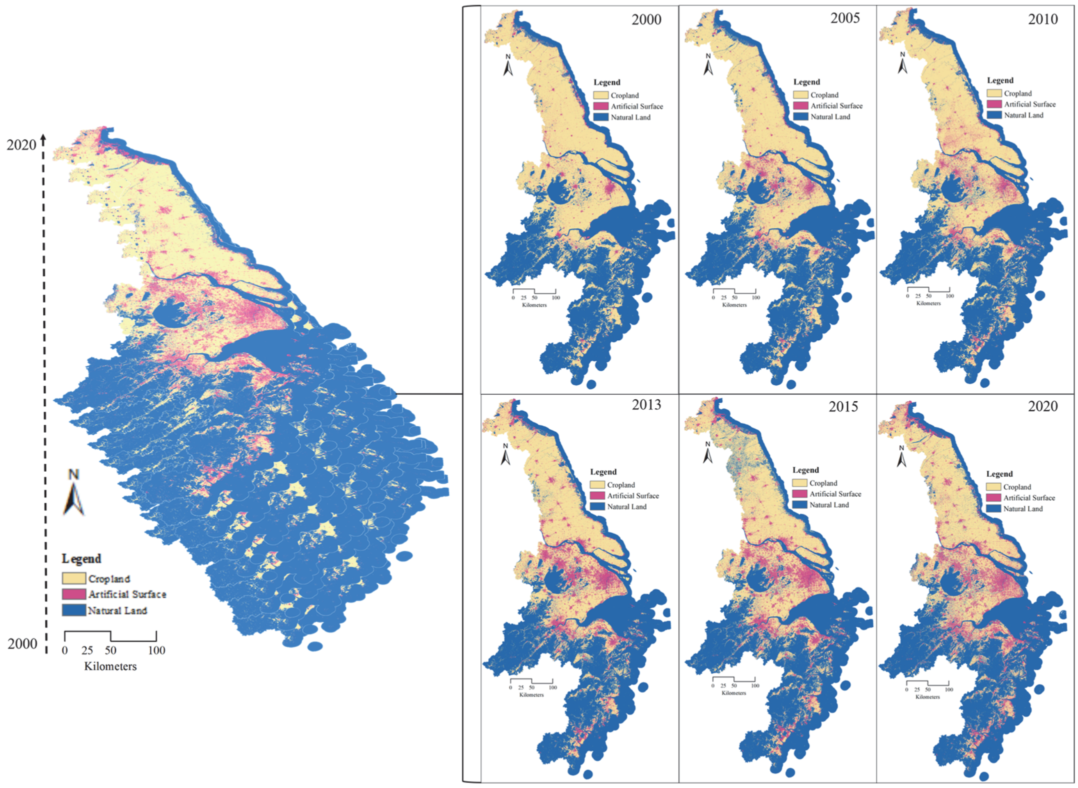

Figure 3. Spatial distribution of year-by-year land use types from 2000 to 2020.

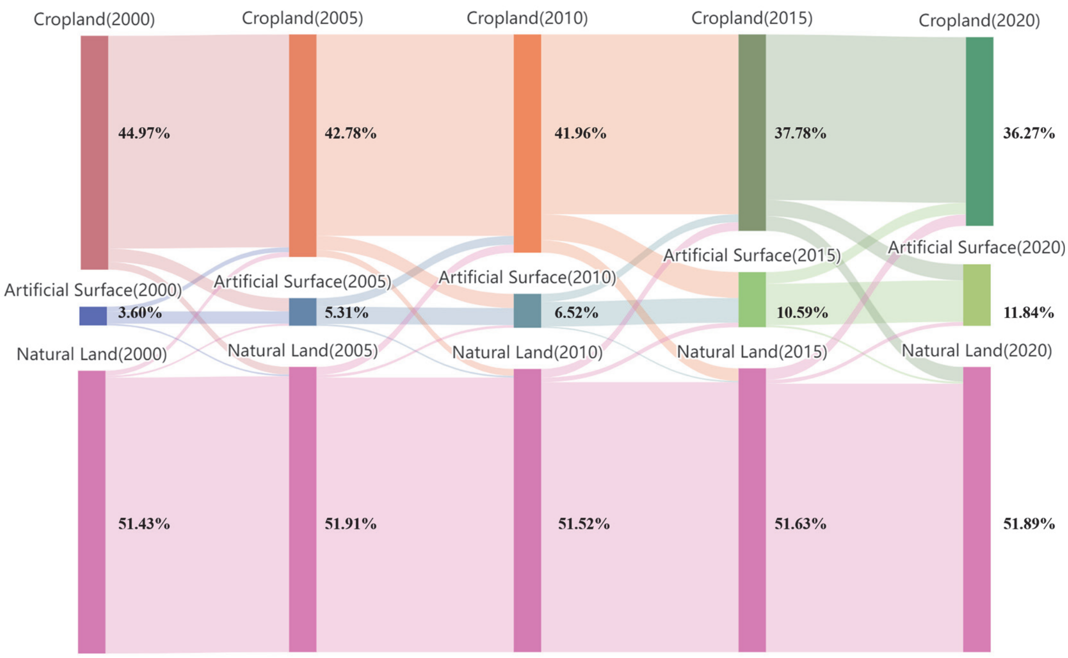

Figure 4. Conversion of different land use types in the coastal zone of the Yangtze River Delta from 2000 to 2020.

Figure 5 depicts how land use was transferred in the coastal zone of Jiangsu and Zhejiang provinces, as well as Shanghai, during the period 2000–2020. On the one hand, the stacked bar chart intuitively presents the composition and area proportion of land types; on the other hand, the Sankey diagram displays the magnitude of land cover type transfers between different categories. Because the coastal zone of Jiangsu and Shanghai were mostly plains, while hills and mountains dominate the coastal zone of Zhejiang, the proportion of land types in Zhejiang differed significantly from the other two areas. Both Jiangsu and Shanghai had the highest proportion of construction land, while Zhejiang had the highest proportion of natural land. The coastal zone of Jiangsu, Zhejiang and Shanghai all exhibited a significant transfer of land use between the artificial surface and cropland, with Shanghai being the most pronounced. Since 2010, the proportion of cropland in Shanghai has shown a clear downward trend, while the proportion of the artificial surface has increased significantly. In Jiangsu, a certain proportion of cropland was converted to the artificial surface each year, peaking during 2010–2015 and weakening after 2015. The land use change in Zhejiang's coastal zone was less drastic than that of Jiangsu and Shanghai. The cropland area continuously decreased; it was mainly converted into artificial surface.

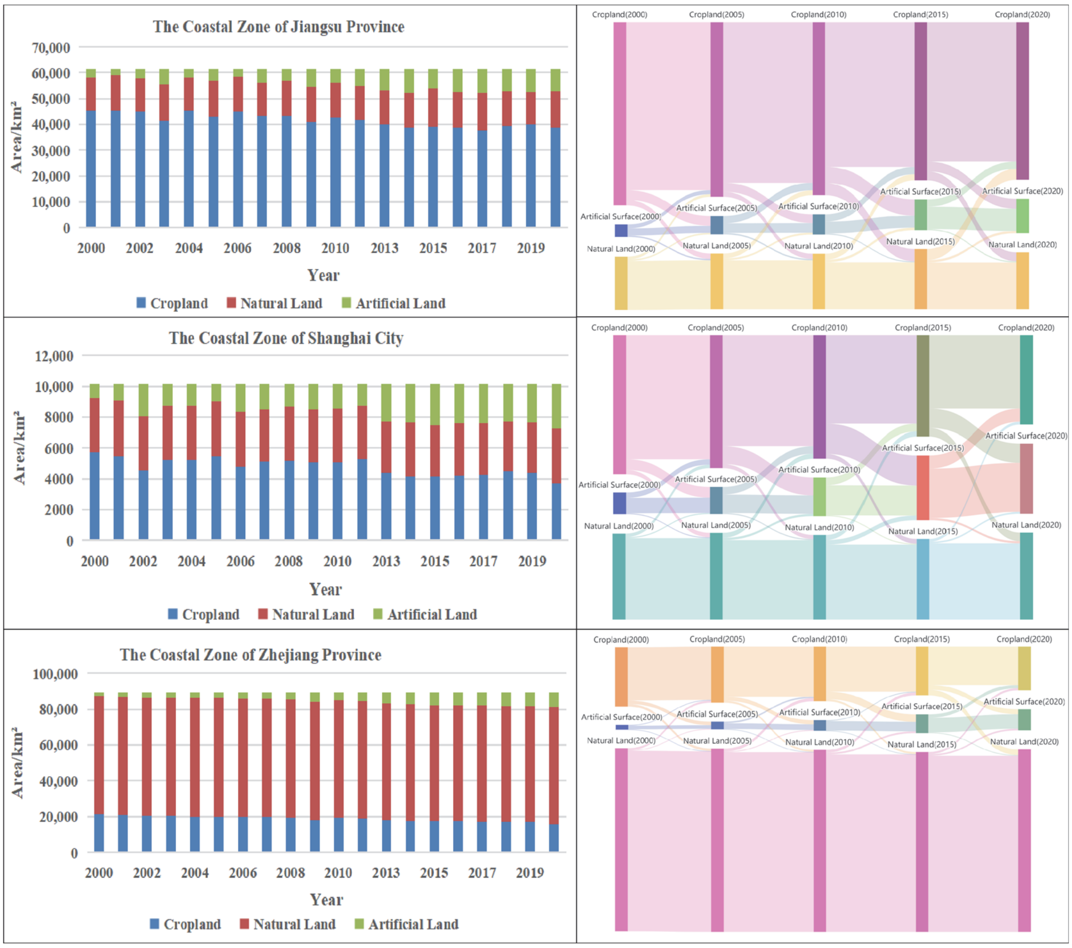

Figure 5. Conversion of land use types in the coastal zone of Jiangsu province, Shanghai city and Zhejiang province from 2000 to 2020.

3.2. *Characteristics of Land Use Dynamics in the Coastal Zone*

To measure the land use change intensity of the Yangtze River Delta coastal zone, the dynamic degree index in different time periods was calculated and the results are shown in Figure 6. In the whole coastal zone of the Yangtze River Delta, the dynamic degree of the artificial surface occupied a dominant position from 2000 to 2020, followed by cropland and natural land. Different land use types had different dynamic degrees in different periods time. Artificial land had the largest change intensity in the periods of 2010–2015 and 2000–2005, followed by 2005–2010. The largest change intensity for cropland was during 2010–2015 and 2015–2020. The change intensity for natural land was relatively small, with the largest change in 2015–2020.

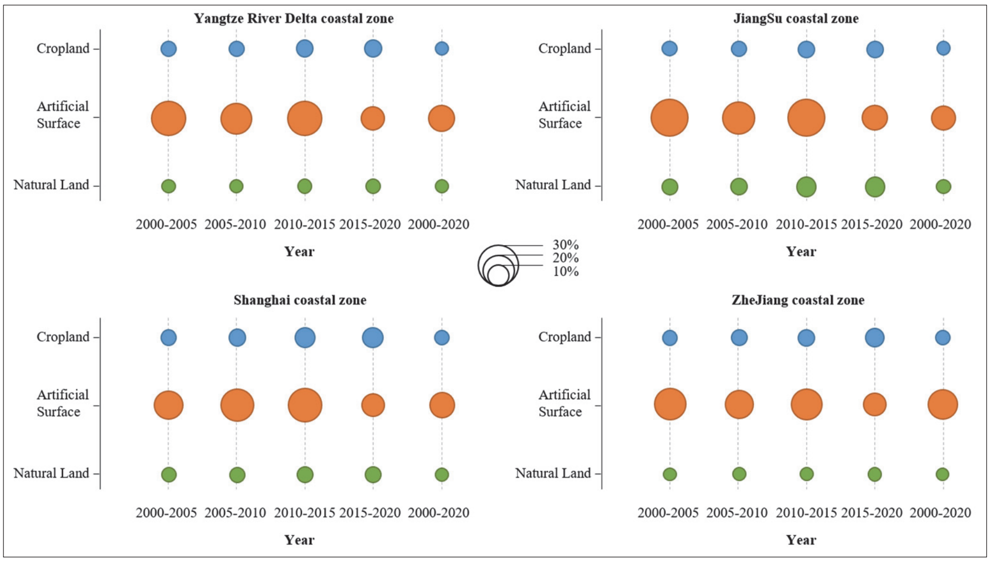

Figure 6. Characteristics of land use dynamics in the Yangtze River Delta coastal zone, 2000–2020.

The land use type with the largest change intensity in the coastal zone of Jiangsu, Shanghai and Zhejiang was artificial surface, and the largest change was in Zhejiang, followed by Shanghai. The periods with the largest change intensity in Zhejiang were 2000–2005 and 2010–2015, in Shanghai, 2005–2010 and 2010–2015, and in Jiangsu, the periods 2000–2005 and 2010–2015. The land use type with the second largest change intensity in Jiangsu was natural land, while in Shanghai and Zhejiang it was cropland, with less change in natural land. This showed that the expansion of artificial land in Jiangsu has encroached on relatively less natural land, while the expansion of artificial land in Shanghai and Zhejiang has encroached on more cropland.

3.3. Analysis of Cropland Loss and Ecological Degradation in the Coastal Zone

Under the influence of urbanization, industrialization and the advancement of marine strategies, land use in the Yangtze River Delta coastal zone has developed increasingly, and its spatial form has evolved from a self-organized natural state to a reorganized state under human control. In order to identify the spatiotemporal evolution pattern of cropland loss and ecological degradation caused by construction and development in the Yangtze River Delta coastal zone, this paper used a 1km grid to spatially divide and merge the areas of three types of land cover and analyzed the evolution process of these three types of land cover through cluster analysis. The results are shown in Figure 7.

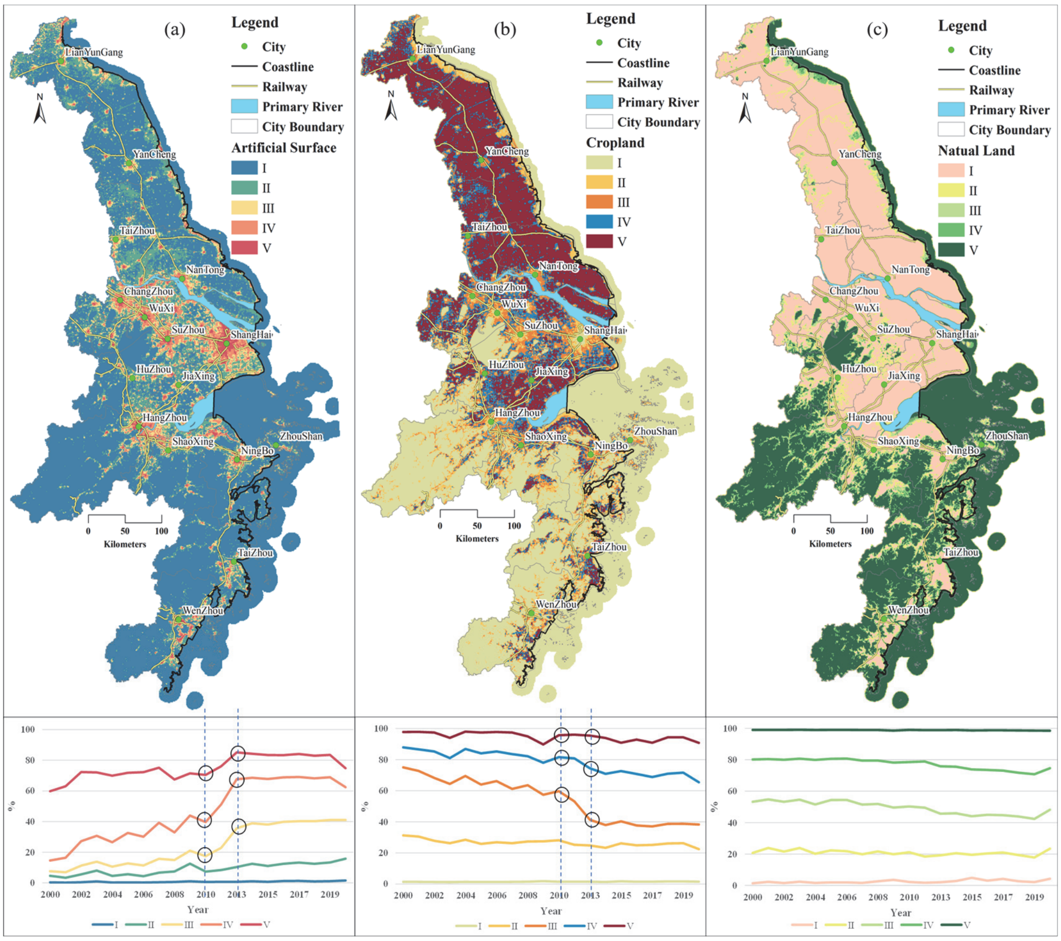

Figure 7. Evolution patterns of artificial surface, cropland and natural land in the coastal zone of the Yangtze River Delta. (**a**) Evolution pattern of artificial surface; (**b**) Evolution pattern of cropland; (**c**) Evolution pattern of natural land.

Figure 7a shows the clustering results of the proportion of the artificial surface area. It can be seen from the change curves of the proportion of each type that, except for type I, the proportion of artificial surface in each category showed an increasing trend. Among these, types III and IV experienced the most significant expansion, with their development intensities increasing from 7.62% and 14.59% in 2000 to 41.03% and 62.41% in 2020, with average annual growth rates of 1.67% and 2.39%, respectively. The period from 2010 to 2013 was particularly characterized by a leap in expansion speed. Types III and IV mainly corresponded to the expansion areas around major cities, while type V represented the downtown areas of major cities. Figure 7b shows the clustering results of the proportion of cropland area, and most of the clustering types showed a decreasing trend. Type III (orange) showed the most significant decrease, with the proportion of corresponding cropland area decreasing from 75.02% in 2000 to 38.23% in 2020, a decrease of more than 50%, especially plummeting from 2010 to 2013. These areas also witnessed a rapid expansion of artificial surface, indicating that the expansion of artificial surface causes the decrease in cropland area. Figure 7c shows the clustering results of the proportion of natural land area and, compared with artificial surface and cropland, the changes in the proportion of different types of natural land cover were relatively small. However, types II, III, and IV still exhibited a slow downward trend over time.

According to the clustering results, the conversion of cropland into artificial surface due to urban expansion was the most common type of land use change. The Yangtze River Delta had three modes of artificial surface expansion: vertically, along the shoreline as the axis, expanding to the sea, and inland in both directions. Artificial surface has expanded inland along almost the entire coastline of the Yangtze River Delta, mainly in cities such as Shanghai, Suzhou, Jiaxing, Huzhou, Hangzhou, Shaoxing, Ningbo, Taizhou and Wenzhou. In contrast, the expansion of artificial surface towards the sea was mainly manifested in cities such as Yancheng, Nantong and Ningbo. Horizontally, artificial surface expanded outward along the banks of the Yangtze River and Qiantang River, and especially significant expansion occurred south of the Yangtze River, mainly in cities such as Shanghai, Suzhou, Nantong, Wuxi, Ningbo, Hangzhou and Jiaxing. The most intense expansion of artificial surface occurred gradually along the central urban areas and essential transportation axes, and the most significant expansion occurred in cities along the Shanghai–Nanjing intercity railway, such as Shanghai, Suzhou, Wuxi and Changzhou, and cities along the Hangzhou–Ningbo high-speed railway, such as Hangzhou, Shaoxing and Ningbo. The expansion of artificial surface was interconnected and influenced by transportation, resulting in a multi-centered urban agglomeration, with the cities connected by a complex and efficient transportation system. This expansion had occupied a large amount of cropland, leading to a significant reduction in cropland area. The expansion of artificial surface has resulted in the fragmentation of cropland patches that were once connected, especially severe in Zhejiang Province and Shanghai, where cropland was scattered throughout the entire region. Over time, these scattered patches gradually became more evident.

To further analyze the impact of artificial surface expansion on natural land, the natural land was subdivided into three categories, forest land, water and unused land, for which the area ratios were calculated and spatiotemporal evolution clustering was analyzed. The clustering results are shown in Figure 8. Figure 8a displays the clustering results of the forest land area ratio, in which the magnitude of change in each type of forest land was relatively small, among which types II, III and IV still exhibited a slow downward trend over time. Figure 8b shows the clustering results of the water area ratio, among which types II, III and IV showed a downward trend, especially type III, which decreased from 53.82% in 2000 to 36.82% in 2020, a decrease of 17%. These areas are mainly located near the coastline, including Lianyungang, Yancheng, Ningbo, Zhoushan, Taizhou, Wenzhou and Shanghai, mainly due to land reclamation and sediment deposition that has extended the shoreline. Figure 8c shows the clustering results of the unused land area ratio. Overall, the trend could be described as first increasing and then decreasing, with 2011 as the watershed year. Before 2011, there was an increasing trend, especially for type V, which mainly represents newly added coastal wetlands after land reclamation that led to shoreline migration, located near the coastline of cities such as Lianyungang, Yancheng, Nantong, Shanghai and Ningbo. After 2011, there was a decreasing trend, manifested by the degradation of coastal wetlands into artificial surface. The interaction between artificial surface, water and unused land in the coastal zones was relatively intricate, where the expansion of the artificial surface led to a decrease in coastal unused land (wetlands), which in turn caused a decrease in water due to shoreline migration, and the migrated part became newly added unused land (wetlands).

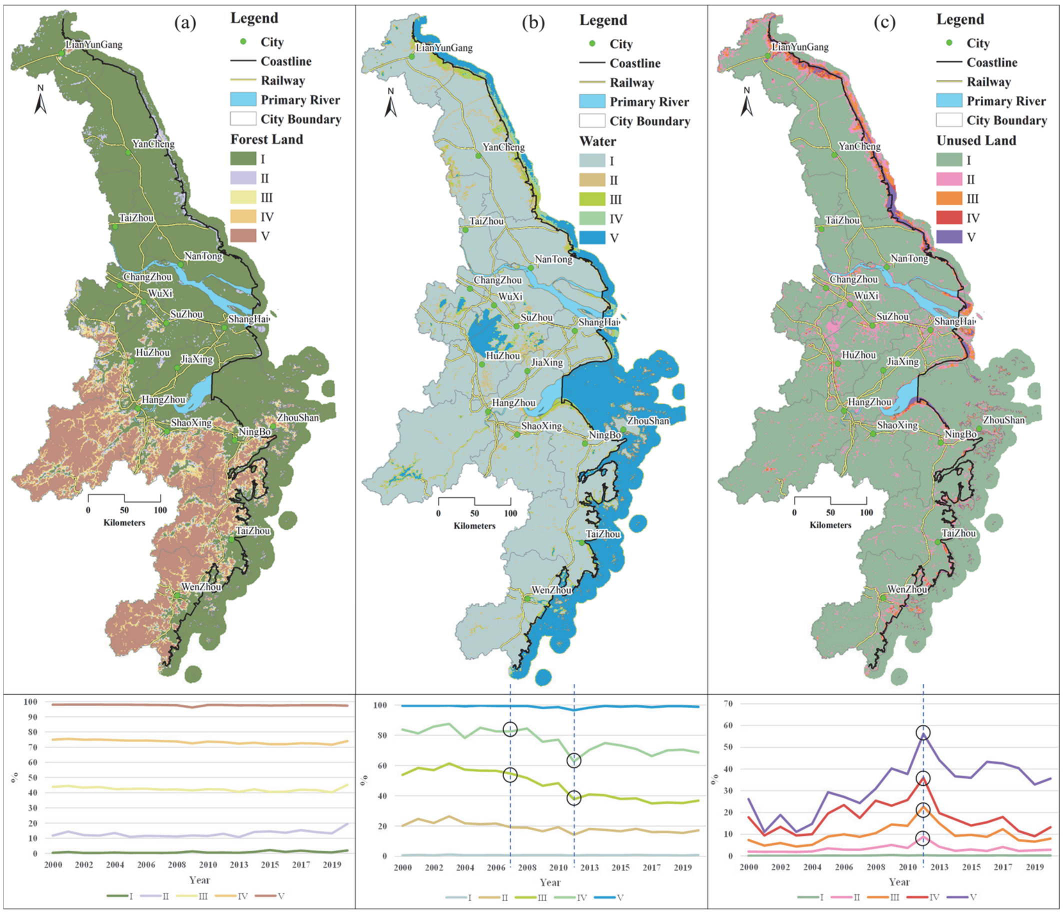

Figure 8. Evolution patterns of forest land, water and unused land in the coastal zone of the Yangtze River Delta. (**a**) Evolution pattern of forest land; (**b**) Evolution pattern of water; (**c**) Evolution pattern of unused land.

4. Discussion

4.1. Land Use Evolution Analysis

The Yangtze River Delta coastal zone epitomized the strong interaction between global change and human activities. Under the background of increasingly deepening coastal development and policy support, land use changes in this area have intensified, making the area demonstrate a variety of conflicts between artificial surface expansion, cropland protection and natural land conservation. Analyzing the evolution of land use patterns in the coastal zone is of paramount significance for boosting the development of the Yangtze River Delta coastal zone. This paper selected the land use types in the entire Yangtze River Delta coastal zone over a period of 20 years for the study of artificial surface expansion, cropland loss and ecological degradation, as well as the long-term evolution trend. In terms of quantity and structure, land use changes showed a trend of a sustained and rapid increase in the artificial surface, the continuous loss of cropland, and slight changes in natural land, with fluctuations. These findings were consistent with those of other studies [36,43,44]. The above studies focused more on the temporal and spatial evolution of the overall pattern and were unable to discover the local characteristics of temporal and spatial evolution. In this paper, grid segmentation and spatiotemporal clustering methods were used to discover local spatial and temporal evolution characteristics. For example, the main areas and critical change points of cropland loss, the serious areas and duration of ecological degradation, etc., could be obtained from corresponding spatiotemporal clustering types.

4.2. Selection of Cluster Number and Grid Size

This paper adopted a spatiotemporal clustering algorithm based on the FCM algorithm for spatiotemporal evolution analysis, which can realize the spatiotemporal expression and comparative analysis of multiple time series land use data. The FCM algorithm quantifies some indicators with unclear boundaries or fuzzy definitions and converts these difficult-to-quantify indicators into quantifiable indicators through a fuzzy function, making the evaluation process more reasonable and accurate; meanwhile, its calculation is fast, which is one of its advantages. The main parameters that affected the results of the clustering analysis of land use evolution were the number of clusters and the grid size. To determine the number of clusters, the fuzzy partition coefficient and continuous experimentation were mainly adopted. When there are slight differences in the time series curves of certain categories, we consider combining these types to reduce the number of clusters. When the study area is finally divided into five categories, the time series curves display good differences.

In terms of grid size, taking the evolution analysis of cultivated land as an example, we found that a 500 m grid size leads to a huge amount of data (666,754 grids), resulting in very long clustering times and many fragments and isolated points, which are not conducive to the analysis of the overall spatiotemporal pattern of the evolution, as shown in Figure 9a. When the grid size is greater than or equal to 5 km (7086 grids), many layout details disappear, as shown in Figure 9b; comparatively, a grid size of 1–2 km (168,070 and 42,626 grids, respectively) in length is a relatively moderate and typical research scale, which can capture the local details of changes and grasp the overall spatial characteristics from a global perspective, as shown in Figure 9c. A 1 km grid size retains more local detail features relative to 2 km, and in combination with previous research experience [34,37,45], so this paper used a 1 km grid length for the clustering analysis of land use spatiotemporal evolution. However, there is currently no unified grid size selection standard, and the changes in information caused by grid size changes still require further research.

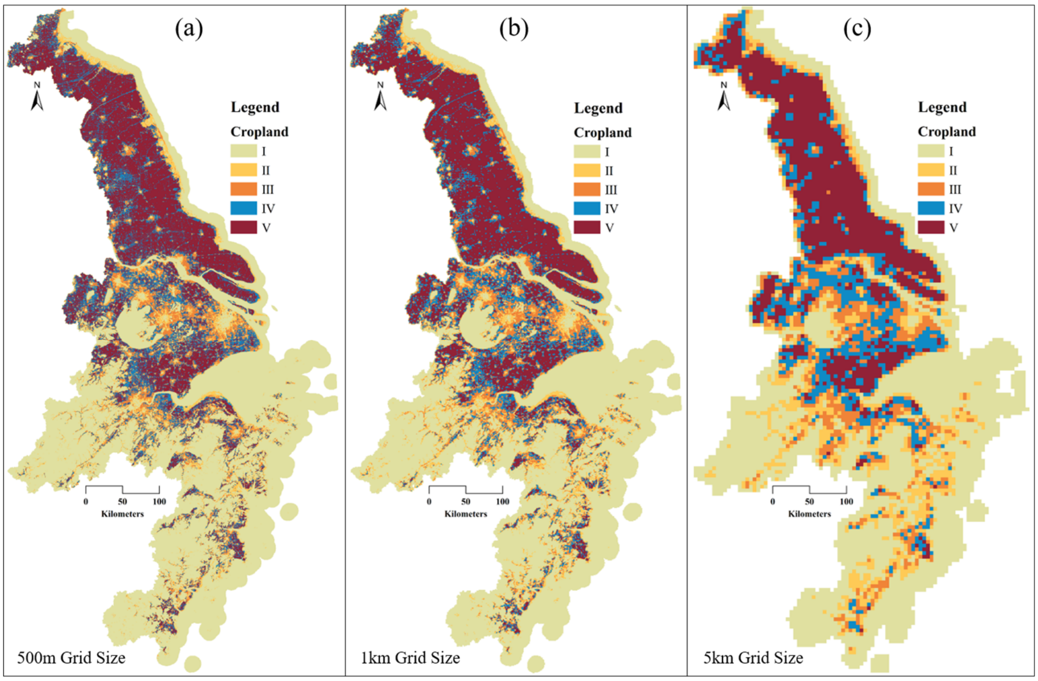

Figure 9. Evolution patterns of cropland under different grid sizes. (**a**) Evolution pattern of cropland under 500 m grid size; (**b**) Evolution pattern of cropland under 1km grid size; (**c**) Evolution pattern of cropland under 5 km grid size.

5. Conclusions

Based on 20 years of Landsat images from the GEE platform, the time series land use in the coastal zone of the Yangtze River Delta in China was classified. Then, a spatiotemporal clustering method based on grid segmentation was proposed to analyze the spatiotemporal evolution details of artificial surface expansion and the risks of cropland loss and ecological degradation caused by it. The results showed that significant changes have taken place in the quantitative structure and spatial morphology of coastal land use in the past 20 years. The artificial surface maintained a growth trend, increasing by 229%, while cropland decreased by 19%. Natural land showed a fluctuation pattern of "up→down→up". Artificial surface mainly undergoes a progressive spatial expansion along the central urban area and important transportation axes (types III and IV), with the most dramatic changes occurring from 2010 to 2013. Category III cropland loss was the most significant, falling from 75.02% in 2000 to 38.23% in 2020. At the same time, the change in the type III water body corresponds to the newly increased area of reclamation, which has decreased by 17% in the past 20 years, indicating that the degradation of coastal natural wetlands was significant.

This paper highlights the potential of the GEE platform and long-term remote sensing image data in identifying the dynamic characteristics and detailed rules of land use evolution in the coastal zone, such as the evolution mode, spatial distribution and change point. This knowledge, teeming with details, helps us to understand the general rules of human expansion activities in the coastal zone so that we can develop more targeted and differentiated policies for coastal zone development and protection. Furthermore, the research methodology and approach can be applied to analyze land use in different scenarios, which also helps the process and mechanism of human activity impacts, thus unleashing the application potential of long-term time series remote sensing big data.

Author Contributions: Conceptualization, L.Y. and Y.W.; formal analysis, L.Y., C.S. and Y.Y.; funding acquisition, L.Y.; methodology, Y.W., L.Y. and Y.Y.; writing—original draft, and writing—review and editing, L.Y., Y.W., C.S. and Y.Y. All authors have read and agreed to the published version of the manuscript.

Funding: This paper was supported by Zhejiang Provincial Natural Science Foundation of China under Grant No. LTGG23D010002; the National Natural Science Foundation of China under Grant No.41801297; Open Funds of Key Laboratory of Ocean Space Resource Management Technology, MNR (KF-2021-102); Science Foundation of Zhejiang Sci-Tech University (ZSTU) under Grant No.20032312-Y.

Data Availability Statement: Not applicable.

Conflicts of Interest: The authors declare no conflict of interest.

References

1. Ramesh, R.; Chen, Z.; Cummins, V.; Day, J.; D'Elia, J.; Dennison, B.; Forbes, D.L.; Glaeser, B.; Glaser, M.; Glavovic, B.; et al. Land–ocean interactions in the coastal zone: Past, present & future. *Anthropocene* **2015**, *12*, 85–98.
2. Halpern, B.S.; Frazier, M.; Afflerbach, J.; Lowndes, J.S.; Micheli, F.; O'Hara, C.; Scarborough, C.; Selkoe, K.A. Recent pace of change in human impact on the world's ocean. *Sci. Rep.* **2019**, *9*, 11609. [CrossRef] [PubMed]
3. He, Q.; Silliman, B.R. Climate change, human impacts, and coastal ecosystems in the Anthropocene. *Curr. Biol.* **2019**, *29*, R1021–R1035. [CrossRef] [PubMed]
4. Du, P.P.; Hou, X.Y.; Xu, H. Dynamic Expansion of Urban Land in China's Coastal Zone since 2000. *Remote Sens.* **2022**, *14*, 916. [CrossRef]
5. Goldberg, L.; Lagomasino, D.; Thomas, N.; Fatoyinbo, T. Global declines in human-driven mangrove loss. *Glob. Change Biol.* **2020**, *26*, 5844–5855. [CrossRef] [PubMed]
6. Abdullah, A.Y.M.; Masrur, A.; Adnan, M.S.G.; Baky, M.; Al, A.; Hassan, Q.K.; Dewan, A. Spatio-temporal patterns of land use/land cover change in the heterogeneous coastal region of Bangladesh between 1990 and 2017. *Remote Sens.* **2019**, *11*, 790. [CrossRef]
7. Mentaschi, L.; Vousdoukas, M.I.; Pekel, J.F.; Voukouvalas, E.; Feyen, L. Global long-term observations of coastal erosion and accretion. *Sci. Rep.* **2018**, *8*, 12876. [CrossRef]

8. Amani, M.; Ghorbanian, A.; Ahmadi, S.A.; Kakooei, M.; Moghimi, A.; Mirmazloumi, S.M.; Moghaddam, S.H.A.; Mahdavi, S.; Ghahremanloo, M.; Parsian, S.; et al. Google earth engine cloud computing platform for remote sensing big data applications: A comprehensive review. *IEEE J. Sel. Top. Appl. Earth Obs. Remote Sens.* **2020**, *13*, 5326–5350. [CrossRef]
9. Chamberlain, D.A.; Phinn, S.R.; Possingham, H.P. Mangrove forest cover and phenology with landsat dense time series in central queensland, Australia. *Remote Sens.* **2021**, *13*, 3032. [CrossRef]
10. Cao, W.; Zhou, Y.; Li, R.; Li, X. Mapping changes in coastlines and tidal flats in developing islands using the full time series of Landsat images. *Remote Sens. Environ.* **2020**, *239*, 111665. [CrossRef]
11. Kuenzer, C.; Bluemel, A.; Gebhardt, S.; Quoc, T.V.; Dech, S. Remote sensing of mangrove ecosystems: A review. *Remote Sens.* **2011**, *3*, 878–928. [CrossRef]
12. Gallant, A.L. The challenges of remote monitoring of wetlands. *Remote Sens.* **2015**, *7*, 10938–10950. [CrossRef]
13. Duan, Y.Q.; Tian, B.; Li, X.; Liu, D.; Sengupta, D.; Wang, Y.; Peng, Y. Tracking changes in aquaculture ponds on the China coast using 30 years of Landsat images. *Int. J. Earth Obs.* **2021**, *102*, 102383. [CrossRef]
14. Huang, B.Q.; Huang, J.L.; Pontius, R.G., Jr.; Tu, Z. Comparison of Intensity Analysis and the land use dynamic degrees to measure land changes outside versus inside the coastal zone of Longhai, China. *Ecol. Indic.* **2018**, *89*, 336–347. [CrossRef]
15. Jia, M.M.; Wang, Z.M.; Zhang, Y.Z.; Mao, D.H.; Wang, C. Monitoring loss and recovery of mangrove forests during 42 years: The achievements of mangrove conservation in China. *Int. J. Earth Obs.* **2018**, *73*, 535–545. [CrossRef]
16. Tian, B.; Wu, W.T.; Yang, Z.Q.; Zhou, Y.X. Drivers, trends, and potential impacts of long-term coastal reclamation in China from 1985 to 2010. *Estuar. Coast. Shelf Sci.* **2016**, *170*, 83–90. [CrossRef]
17. Shi, X.Y.; Matsui, T.; Haga, C.; Machimura, T.; Hashimoto, S.; Saito, O. A scenario-and spatial-downscaling-based land-use modeling framework to improve the projections of plausible futures: A case study of the Guangdong–Hong Kong–Macao Greater Bay Area, China. *Sustain. Sci.* **2021**, *16*, 1977–1998. [CrossRef]
18. Lin, W.P.; Cen, J.W.; Xu, D.; Du, S.Q.; Gao, J. Wetland landscape pattern changes over a period of rapid development (1985–2015) in the ZhouShan Islands of Zhejiang province, China. *Estuar. Coast. Shelf Sci.* **2018**, *213*, 148–159. [CrossRef]
19. Ding, Z.; Su, F.Z.; Zhang, J.J.; Zhang, Y.; Luo, S.C.; Tang, X.G. Clustering coastal land use sequence patterns along the sea–land direction: A case study in the coastal zone of Bohai Bay and the Yellow River Delta, China. *Remote Sens.* **2019**, *11*, 2024. [CrossRef]
20. Zhang, X.; Xiao, X.; Wang, X.; Xu, X.; Chen, B.; Wang, J.; Ma, J.; Zhao, B.; Li, B. Quantifying expansion and removal of Spartina alterniflora on Chongming island, China, using time series Landsat images during 1995–2018. *Remote Sens. Environ.* **2020**, *247*, 111916. [CrossRef]
21. Zhou, Z.M.; Yang, Y.M.; Chen, B.Q. Estimating the Spartina alterniflora fractional vegetation cover using high spatial resolution remote sensing in a coastal wetland. *Acta Ecol. Sin.* **2017**, *37*, 505–512.
22. Li, W.; El-Askary, H.; Qurban, M.A.; Li, J.; ManiKandan, K.P.; Piechota, T. Using multi-indices approach to quantify mangrove changes over the Western Arabian Gulf along Saudi Arabia coast. *Ecol. Indic.* **2019**, *102*, 734–745. [CrossRef]
23. Xiao, H.; Su, F.; Fu, D.; Wang, Q.; Huang, C. Coastal mangrove response to marine erosion: Evaluating the impacts of spatial distribution and vegetation growth in Bangkok Bay from 1987 to 2017. *Remote Sens.* **2020**, *12*, 220. [CrossRef]
24. Yan, J.; Zhao, S.; Su, F.; Du, J.; Feng, P.; Zhang, S. Tidal Flat Extraction and Change Analysis Based on the RF-W Model: A Case Study of Jiaozhou Bay, East China. *Remote Sens.* **2021**, *13*, 1436. [CrossRef]
25. Santos, R.O.; Lirman, D.; Pittman, S.J. Long-term spatial dynamics in vegetated seascapes: Fragmentation and habitat loss in a human-impacted subtropical lagoon. *Mar. Ecol.* **2016**, *37*, 200–214. [CrossRef]
26. Xu, C.; Zhou, C.; Ma, K.; Wang, P.; Yue, X. Response of water environment to land reclamation in Jiaozhou Bay, China over the last 150 years. *Front. Mar. Sci.* **2021**, *8*, 750288. [CrossRef]
27. Wan, L.; Liu, H.Y.; Gong, H.B.; Ren, Y.J. Effects of climate and land use changes on vegetation dynamics in the Yangtze River Delta, China based on abrupt change analysis. *Sustainability* **2020**, *12*, 1955. [CrossRef]
28. Wang, Q.; Xu, Y.P.; Xu, Y.; Wu, L.; Wang, Y.F.; Han, L.F. Spatial hydrological responses to land use and land cover changes in a typical catchment of the Yangtze River Delta region. *Catena* **2018**, *170*, 305–315. [CrossRef]
29. Yu, M.; Yang, Y.J.; Chen, F.; Zhu, F.W.; Qu, J.F.; Zhang, S.L. Response of agricultural multifunctionality to farmland loss under rapidly urbanizing processes in Yangtze River Delta, China. *Sci. Total. Environ.* **2019**, *666*, 1–11. [CrossRef]
30. Zhang, D.; Wang, X.R.; Qu, L.P.; Li, S.C.; Lin, Y.P.; Yao, R.; Zhou, X.; Li, J.Y. Land use/cover predictions incorporating ecological security for the Yangtze River Delta region, China. *Ecol. Indic.* **2020**, *119*, 106841. [CrossRef]
31. Lin, M.X.; Lin, T.; Sun, C.G.; Jones, L.; Sui, J.L.; Zhao, Y.; Liu, J.K.; Xing, L.; Ye, H.; Zhang, G.Q.; et al. Using the Eco-Erosion Index to assess regional ecological stress due to urbanization–A case study in the Yangtze River Delta urban agglomeration. *Ecol. Indic.* **2020**, *111*, 106028. [CrossRef]
32. Zhang, S.Y.; Shao, H.Y.; Li, X.Q.; Xian, W.; Shao, Q.F.; Yin, Z.Q.; Lai, F.; Qi, J.G. Spatiotemporal Dynamics of Ecological Security Pattern of Urban Agglomerations in Yangtze River Delta Based on LUCC Simulation. *Remote Sens.* **2022**, *14*, 296. [CrossRef]
33. Fan, J. Draft of major function oriented zoning of China. *Acta Geogr. Sin.* **2015**, *70*, 186–201.
34. Wang, M.M.; Zhang, H.Y.; Zhang, Y.G.; Lin, M.S.; Gong, P. Evolution analysis of land use pattern in the Changjiang River Delta coastal zone in recent 39 years. *Haiyang Xuebao* **2020**, *42*, 142–154.
35. Li, M.N.; Yin, P.; Duan, X.Y.; Liu, J.Q.; Qiu, J.D.; Phung, V.P. Land-use changes and human driving in and near the Yangtze River delta from 1995–2015. *J. Ocean. Univ. China* **2018**, *17*, 1361–1368. [CrossRef]

36. Sun, W.; Shan, J.; Wang, Z.M.; Wang, L.; Lu, D.M.; Jin, Z.F.; Yu, K. Geospatial analysis of urban expansion using remote sensing methods and data: A case study of Yangtze River Delta, China. *Complexity* **2020**, *2020*, 3239471. [CrossRef]
37. Wang, Y.F.; He, Y.; Li, J.Y.; Jiang, Y.Z. Evolution Simulation and Risk Analysis of Land Use Functions and Structures in Ecologically Fragile Watersheds. *Remote Sens.* **2022**, *14*, 5521. [CrossRef]
38. Liu, J.Y.; Ning, J.; Kuang, W.H.; Xu, X.L.; Zhang, S.W.; Yan, C.Z.; Li, R.D.; Wu, S.X.; Hu, Y.F.; Du, G.M.; et al. Spatio-temporal patterns and characteristics of land-use change in China during 2010-2015. *Acta Geogr. Sin.* **2018**, *73*, 789–802.
39. Cheng, W.M.; Gao, X.Y.; Ma, T.; Xu, X.L.; Chen, Y.J.; Zhou, C.H. Spatial-temporal distribution of cropland in China based on geomorphologic regionaliza-tion during 1990–2015. *Acta Geogr. Sin.* **2018**, *73*, 1613–1629.
40. Dunn, J.C. A fuzzy relative of the ISODATA process and its use in detecting compact well-separated clusters. *J. Cybern.* **1973**, *3*, 32–57. [CrossRef]
41. Bezdek, J.C. *Pattern Recognition with Fuzzy Objective Function Algorithms*; Plenum Press: New York, NY, USA, 1983.
42. Taylor, S.J.; Letham, B. Forecasting at scale. *Am. Stat.* **2018**, *72*, 37–45. [CrossRef]
43. Chen, W.X.; Zhao, H.B.; Li, J.F.; Zhu, L.J.; Wang, Z.Y.; Zeng, J. Land use transitions and the associated impacts on ecosystem services in the Middle Reaches of the Yangtze River Economic Belt in China based on the geo-informatic Tupu method. *Sci. Total. Environ.* **2020**, *701*, 134690. [CrossRef] [PubMed]
44. Wang, X.G.; Yan, F.Q.; Su, F.Z. Changes in coastline and coastal reclamation in the three most developed areas of China 1980–2018. *Ocean. Coast. Manag.* **2021**, *204*, 105542. [CrossRef]
45. Qi, J.C.; Liu, H.P.; Liu, X.P.; Zhang, Y.H. Spatiotemporal evolution analysis of time-series land use change using self-organizing map to examine the zoning and scale effects. *Comput. Environ. Urban.* **2019**, *76*, 11–23. [CrossRef]